Histone Methyltransferase G9a Is Required for Cardiomyocyte Homeostasis and Hypertrophy

BACKGROUND: Correct gene expression programming of the cardiomyocyte underlies the normal functioning of the heart. Alterations to this can lead to the loss of cardiac homeostasis, triggering heart dysfunction. Although the role of some histone methyltransferases in establishing the transcriptional program of postnatal cardiomyocytes during heart development has been shown, the function of this class of epigenetic enzymes is largely unexplored in the adult heart. In this study, we investigated the role of G9a/Ehmt2, a histone methyltransferase that defines a repressive epigenetic signature, in defining the transcriptional program for cardiomyocyte homeostasis and cardiac hypertrophy.

METHODS: We investigated the function of G9a in normal and stressed cardiomyocytes with the use of a conditional, cardiac-specific G9a knockout mouse, a specific G9a inhibitor, and high-throughput approaches for the study of the epigenome (chromatin immunoprecipitation sequencing) and transcriptome (RNA sequencing); traditional methods were used to assess cardiac function and cardiovascular disease.

RESULTS: We found that G9a is required for cardiomyocyte homeostasis in the adult heart by mediating the repression of key genes regulating cardiomyocyte function via dimethylation of H3 lysine 9 and interaction with enhancer of zeste homolog 2, the catalytic subunit of polycomb repressive complex 2, and MEF2C-dependent gene expression by forming a complex with this transcription factor. The G9a-MEF2C complex was found to be required also for the maintenance of heterochromatin needed for the silencing of developmental genes in the adult heart. Moreover, G9a promoted cardiac hypertrophy by repressing antihypertrophic genes.

CONCLUSIONS: Taken together, our findings demonstrate that G9a orchestrates critical epigenetic changes in cardiomyocytes in physiological and pathological conditions, thereby providing novel therapeutic avenues for cardiac pathologies associated with dysregulation of these mechanisms.

Roberto Papait, PhD*
Simone Serio, MSc*
Christina Pagiatakis, PhD*
Francesca Rusconi, PhD
Pierluigi Carullo, MSc
Marta Mazzola, MSc
Nicolò Salvarani, PhD
Michele Miragoli, PhD
Gianluigi Condorelli, MD, PhD

*Drs Papait, Serio, and Pagiatakis contributed equally.

Correspondence to: Roberto Papait, PhD, or Gianluigi Condorelli, MD, PhD, Humanitas Clinical and Research Center, Via Manzoni 56, Rozzano 20089, Milan, Italy. E-mail roberto.papait@humanitasresearch.it, or gianluigi.condorelli@hunimed.eu

Sources of Funding, see page 1245

Key Words: EHMT2 protein, mouse ■ epigenomics ■ heart failure ■ heterochromatin ■ histone methylation ■ hypertrophy ■ MEF2C protein, mouse

Clinical Perspective

What Is New?

- The histone methyltransferase G9a is important in defining the epigenetic landscape that maintains the transcription program of the cardiomyocyte and in regulating gene expression reprogramming during cardiac hypertrophy.
- Impaired G9a function can promote heart dysfunction.

What Are the Clinical Implications?

- G9a may represent a therapeutic target for early stages of cardiac hypertrophy.
- The possibility of using histone methyltransferase inhibitors for the treatment of heart failure requires functional characterization of the molecular targets not only in the disease state but also in the basal condition.

Underlying the correct functioning of the heart is a specific gene expression program, the alteration of which results in heart failure (HF), a leading cause of morbidity and mortality.[1] HF is characterized by de novo expression of genes expressed in the fetal heart. Thus, transcriptional changes contribute to the development of the disease.[2,3] The importance of epigenetics in regulating cardiac gene expression is increasingly recognized.[4]

Histone methylation is an important epigenetic modulator of gene expression, so, not surprisingly, its deregulation can cause developmental defects and diseases.[5] For the heart, it is involved in the maintenance of cardiac homeostasis and hypertrophy. Indeed, PAX-interacting protein 1, an essential cofactor for methylation (me) of histone 3 (H3) at lysine (K) 4, is required for maintenance of the transcriptional program in normal cardiomyocytes (CMs).[6] Moreover, a genome-wide study revealed that trimethylation of H3 at K4, K9, and K27 and dimethylation of H3 at K9 and K79 regulate gene expression reprogramming in pressure-overload hypertrophy.[7] In addition, JMJD2A/KMD4, which catalyzes the demethylation of trimethylated H3 at K9 (H3K9me3) and K36 (H3K36me3), is required for cardiac hypertrophy.[8] JMJD2A acts synergistically with serum response factor and myocardin to regulate FHL1, which is involved in mediating the hypertrophic response.[8,9] However, the factors and mechanisms that determine the histone methylation pattern in CMs under physiological and pathological conditions remain unclear.

G9a (euchromatic histone lysine methyltransferase 2) is a histone methyl-transferase (HMT) belonging to the SET domain-containing family of proteins; it monomethylates and dimethylates K9 (H3K9me1 and H3K9me2) and, to a lesser extent, K27 (H3K27) on histone H3. In vivo, G9a forms a heteromeric complex with G9a-like protein (euchromatic histone lysine methyltransferase 1), another primary enzyme catalyzing methylation at H3K9.[10,11] Genetic analysis showed that the HMT activity of G9a is more important than that of G9a-like protein in vivo and that neither can compensate for loss in the HMT activity of the other.[10,12]

G9a is also a major transcriptional repressor promoting the formation of facultative heterochromatin via deposition of H3K9me2 at docking sites for heterochromatin protein 1[13,14] and regulating the activity of polycomb repressive complex 2 (PRC2), which supports gene silencing via trimethylation of H3K27.[15,16] It is required for defining the gene expression program in processes ranging from the development to maintenance of cellular identity during differentiation.[17–19] The important role of G9a in maintaining cell identity is also supported by its involvement in many human tumors.[20]

Two recent studies have implicated G9a in the development of HF. However, they reported conflicting mechanisms: 1 study described G9a as a prohypertrophic gene involved in silencing the expression of adult cardiac myosin heavy chain in pressure-overloaded mice,[21] and in the other, G9a was viewed as an antihypertrophic gene, the downregulation of which was needed for the expression of fetal genes in cardiac hypertrophy.[22] Thus, we decided to study G9a in normal and stressed CMs with the use of a G9a knockout (KO) mouse. Our findings support a dual role for G9a: in the normal heart, G9a acts in an antihypertrophic manner, whereas in the stressed heart, it promotes hypertrophy.

METHODS

Extended methods are given in the online-only Data Supplement.

Mice

Experiments were performed on male, cardiac-specific, tamoxifen-inducible, conditional G9a KO mice, generated with the cre-lox approach; MerCreMer mice; and wild-type mice (strain C57BL/6J) 8 to 10 weeks of age. Transverse aortic constriction (TAC) was used to generate pressure overload–induced hypertrophy[23] in wild-type mice in which 20 mg/mL BIX-01294 (Cayman Chemical) was used to inhibit G9a. Noninvasive echocardiography was performed with the Vevo 2100 high-resolution imaging platform (VisualSonics). All experiments were performed according to the 2010/63/EU Directive and approved by the ethics committee of Humanitas Research Hospital.

Primary CMs

Primary CMs were isolated from 2-day-old pups with the Neonatal Heart Dissociation Kit. Mechanical cardiac parameters were assessed with an IonOptix system.[24] Whole-cell electrophysiological measurements were performed with

Circulation. 2017;136:1233–1246. DOI: 10.1161/CIRCULATIONAHA.117.028561

standard methods.[25] Short interfering RNA for MEF2C (SASI_Mm01_00092891, Sigma-Aldrich) or a universal scrambled RNA was used at a concentration of 50 nmol/L. Western blotting, coimmunoprecipitation, and gene expression analyses were done with standard techniques.

Chromatin Immunoprecipitation and RNA Sequencing

These analyses were performed on CM-enriched populations isolated from mice. Chromatin immunoprecipitation sequencing (ChIP-seq) libraries were generated with the Ovation Ultralow System V2 1-96 kit (NuGEN). Paired-end sequence reads (length, 100 base pairs) were generated on an Illumina HiSeq2500, with each sample containing >30 million reads. RNA sequencing (RNA-seq) libraries were obtained with a ScriptSeq kit (Illumina), quantified with a Qubit 2.0 fluorometer (Life Technologies), and sequenced with TruSeq kits (Illumina). Paired-end 75-base-pair sequence reads were generated (NextSeq, 500Illumina), with each sample containing >50 million reads.

Statistical Analysis

All sequencing experiments were performed on duplicates. GraphPad Prism or R Statistical was used for statistical analyses, THOR for differential peaks calling, and Ingenuity Pathway Analysis for pathway analyses. Two groups were analyzed with the unpaired *t* test; ANOVA was used for experiments with >2 independent groups (1 way) and those with 2 between-subjects factors (2 way).

Complete data sets are deposited at the Gene Expression Omnibus Database (accession number GEO:GSE93754).

RESULTS

G9a Is Required for Preserving CM Function

We first assessed the role of G9a in the normal heart, investigating the effect of downregulating this HMT in 2-month-old mouse CMs. To this end, we used a mouse line with conditional, cardiac-specific KO of this gene generated with the Cre-Lox approach, crossing *G9a*$^{f/f}$ mice with α*MHC-MerCreMer* (Cre) mice; the Cre mice were used as controls. Within 4 weeks of inducing the KO with tamoxifen, mice presented with decreased systolic contractility (percent fractional shortening and ejection fraction) and increased left ventricular internal diameter and ratio of left ventricular weight to body weight (Figure 1A and Figure IA in the online-only Data Supplement). Moreover, overall heart size was enlarged, interstitial fibrosis was increased, and hypertrophic markers were upregulated (Figure 1B and 1C and Figure IB in the online-only Data Supplement). CMs isolated from G9a-KO mice had decreased contractility (Figure 1D) and altered calcium handling; indeed, G9a-KO CMs had significant decreases in calcium parameters such as transient magnitude, departure velocity, and Ca^{2+} reuptake (Figure 1E through 1G). Of note, the Ca^{2+} current was increased (Figure 1H). Thus, G9a is required for correct cardiac functioning in normal, unstressed conditions, and its depletion in CMs impairs contractility and calcium handling.

We then investigated the molecular mechanism of the involvement of G9a in heart homeostasis by first determining the gene expression signature defined by the HMT in CMs. To this end, we sequenced total RNA from CM-enriched populations isolated from G9a-KO and Cre mice and compared the 2 expression profiles. There were 397 differentially expressed genes in G9a-KO CMs, with a relative prevalence (61.5%) of upregulated genes (Figure 2A and Table I in the online-only Data Supplement). Gene Ontology analysis showed that these genes are involved in various biological processes and in defining mammalian phenotypes linked to abnormal heart function (Figure 2A). Among the upregulated genes, we found key cardiac hypertrophy genes such as myosin heavy chain 7 (*Myh7*), natriuretic peptide A (*Nppa*), and α-actin-1 (*Acta1*), as well as several calcium signaling genes, including protein kinase A (*PKA*), calsequestrin 1 (*Casq1*), and regulator of calcineurin 1 (*Rcan1*; Figure 2A and Figure IIA in the online-only Data Supplement).

To identify which modulated genes were direct targets of G9a, we examined the distribution of the HMT at those genes. We thus performed ChIP-seq for G9a and H3K9me2, the main histone methylation catalyzed by the HMT, on isolated G9a-KO and Cre CMs, and we considered the best G9a-bound genomic regions as those that underwent a loss or decrease of G9a binding as well as having a lower level of H3K9me2 in G9a-KO CMs. In line with the HMT activity of G9a, the level of H3K9me2 around the G9a peaks was decreased in G9a-KO CMs (Figure 2B); the distribution profiles of H3K9me2 in Cre CMs versus G9a-KO CMs were only weakly correlated (Pearson correlation: 0.29, 0.22, 0.12, and 0.11 for all comparisons between the replicates; Figure IIB in the online-only Data Supplement). We found 113 508 regions with significantly reduced binding of G9a and decreased H3K9me2 deposition (adjusted $P \leq 0.01$), corresponding to 30% of all the genomic regions we found with decreased G9a binding in G9a-KO CMs (Figure 2C and Table II in the online-only Data Supplement). These best G9a-bound genomic regions mapped prevalently to noncoding regions (introns, 31%; intergenic regions, 66%), with enrichment on repetitive elements (long interspersed nuclear elements, long terminal repeats, short interspersed nuclear elements, and simple repeats; Figure IIC in the online-only Data Supplement). This is coherent with a role for G9a in silencing these genetic elements, as reported for postimplantation epiblasts.[16] One hundred forty-eight genes found upregulated in G9a-KO CMs had G9a bound within 10 kilobases from the transcription start site or gene body (Figure 2C and Table III in the

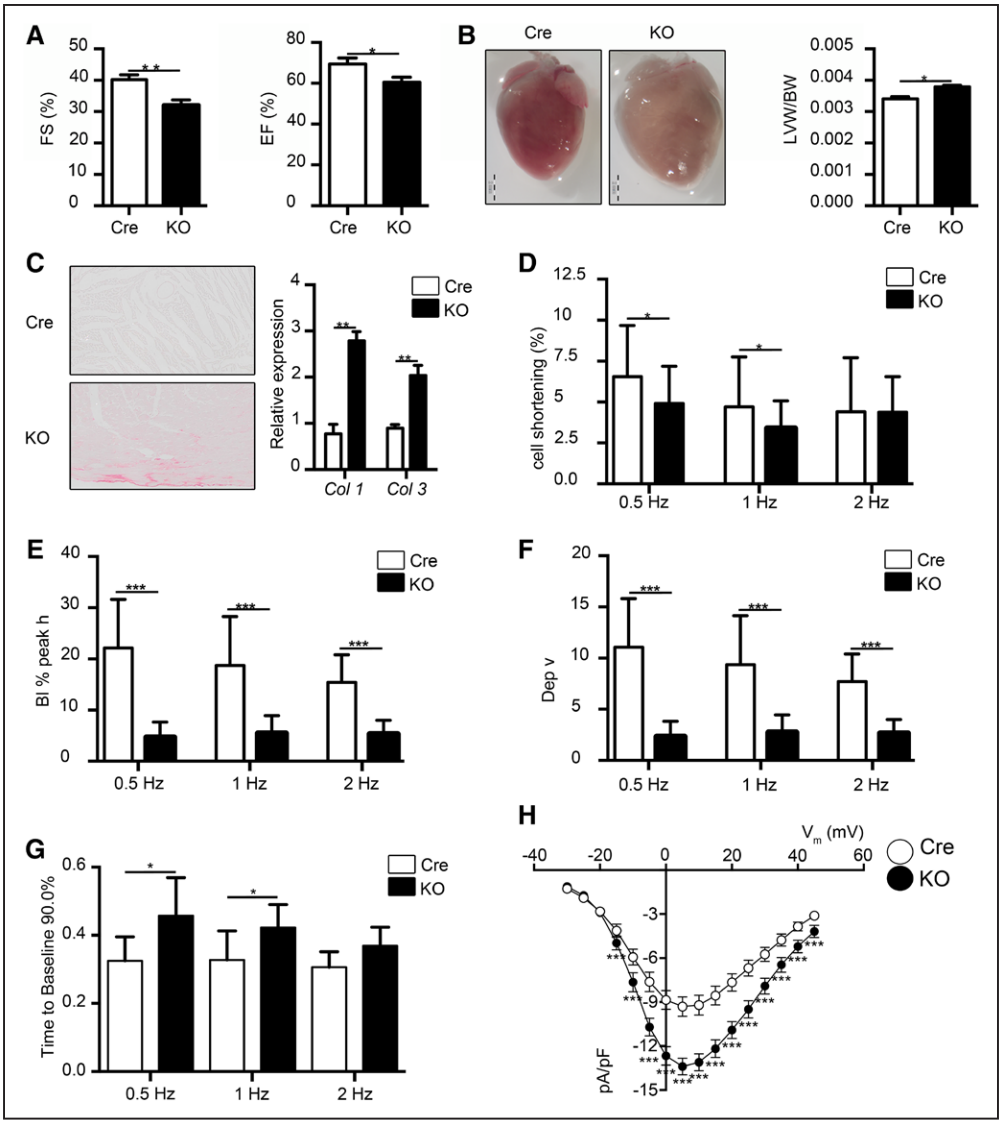

Figure 1. Characterization of cardiac phenotype in G9a$^{f/f}$-αMHC-MerCreMer mice 4 weeks from knockout (KO) induction with tamoxifen.

A, Echocardiographic parameters: percent fractional shortening (FS) and ejection fraction (EF) (mean±SD; n=10). **B**, Representative images of freshly excised whole hearts from Cre and G9a-KO mice (**left**) and the ratio of left ventricular weight to body weight (LVW/BW) (**right**) (mean±SD; n=10). **C**, Assessment of myocardial fibrosis with Picro-Sirius Red staining (**left**) and quantitative real-time polymerase chain reaction analysis of collagen type 1 (*Col1*) and 3 (*Col3*) (**right**) mean±SD; n=3). **D**, Contractility in cardiomyocytes isolated from heart of G9a$^{flox/flox}$-α-MHC-MerCreMer and Cre mice 4 weeks from induction of gene KO (n=12–40 cardiomyocytes). **E** through **G**, Calcium handling parameters: magnitude of transient (BI) (**E**), departure velocity (Dep V) (**F**), and Ca^{2+} reuptake (**G**) in cardiomyocytes isolated from Cre (white bars) and G9a-KO (black bars) mice (n=6–14 cardiomyocytes). **H**, L-type Ca^{2+} current in cardiomyocytes isolated from Cre (white circles) and G9a-KO (black circles) mice (n=12 cardiomyocytes). *P<0.05. **P<0.01. ***P<0.001.

online-only Data Supplement). These included genes of muscle differentiation (eg, *Mef2c*, *Tgfb2*, nebulin [*NEB*], *Myh10*), muscle contraction (eg, myosin binding protein C, fast type [*Mybpc2*], myomesin 2 [*Myom2*]), and calcium ion transport (eg, *Cacnad2d1*). For some of these genes, the changes in transcription and distribution of G9a and H3K9me2 on KO were confirmed by analyzing the profiles obtained by ChIP-seq and RNA-seq (Figure 2D; see also Figures 3C and 4E).

G9a Interacts With PRC2, Regulating Its H3K27 Trimethylation Activity on a Subset of Its Target Genes in Adult CMs

G9a interacts with PRC2, contributing to trimethylation of H3K27 at a set of developmental genes.[15,16] Thus, to assess the relationship between G9a and PRC2 in CMs, we first tested the interaction of G9a with enhancer of zeste homolog 2 (EZH2), the catalytic subunit of PRC2,

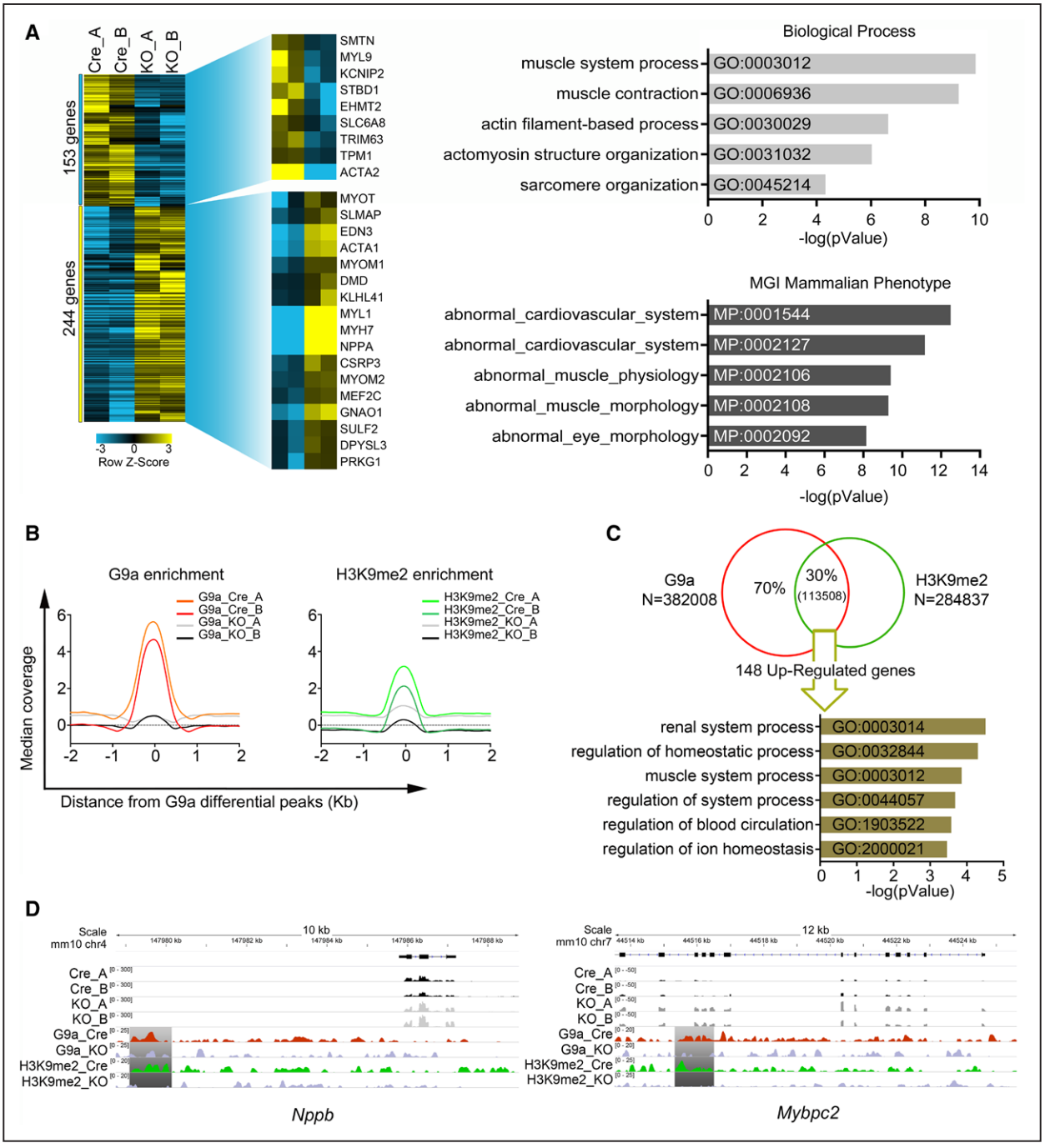

Figure 2. Identification of G9a-targeted genes in normal cardiomyocytes.

A, Heat map of unsupervised hierarchical clustering of 397 genes undergoing a change of expression (log fold change ≥0.5; $P<0.01$; log counts per million ≥1) in cardiomyocytes isolated from G9a$^{flox/flox}$-α-MHC-MerCreMer mice after 4 weeks from knockout (KO) induction with tamoxifen (**left**). Gene ontology (GO) analysis for biological processes and mammalian phenotype of modulated genes (**right**). **B**, Analysis of distribution of H3K9me2 around the genomic regions bound to G9a (±2 kilobases [kb] from peaks). The genome-wide distribution of H3K9me2 was analyzed by chromatin immunoprecipitation sequencing (ChIP-seq) in Cre vs G9a-KO cardiomyocytes. The G9a-bound genomic regions were identified, comparing ChIP-seq for G9a in Cre and G9a-KO cardiomyocytes. **C**, Venn diagram of the overlap between the genomic regions that had a decreased level of G9a in G9a-KO vs Cre cardiomyocytes (G9a differential peaks) with those that had a decreased level of H3K9me2 (H3K9me2 differential peaks) that we considered the best G9a-bound genomic regions. **Arrow** indicates the number of upregulated genes in G9a-KO cardiomyocytes that were associated with the data set of the best G9a-bound genomic regions. Graph shows GO analysis for biological processes of these genes. **D**, RNA sequencing and ChIP-seq profiles for G9a and H3K9me2 on natriuretic peptide B (*Nppb*) and myosin binding protein C, fast type (*Mybpc2*) genes in Cre and G9a-KO cardiomyocytes. The profiles were obtained from the average distribution of reads in replicates normalized to input and library dimension.

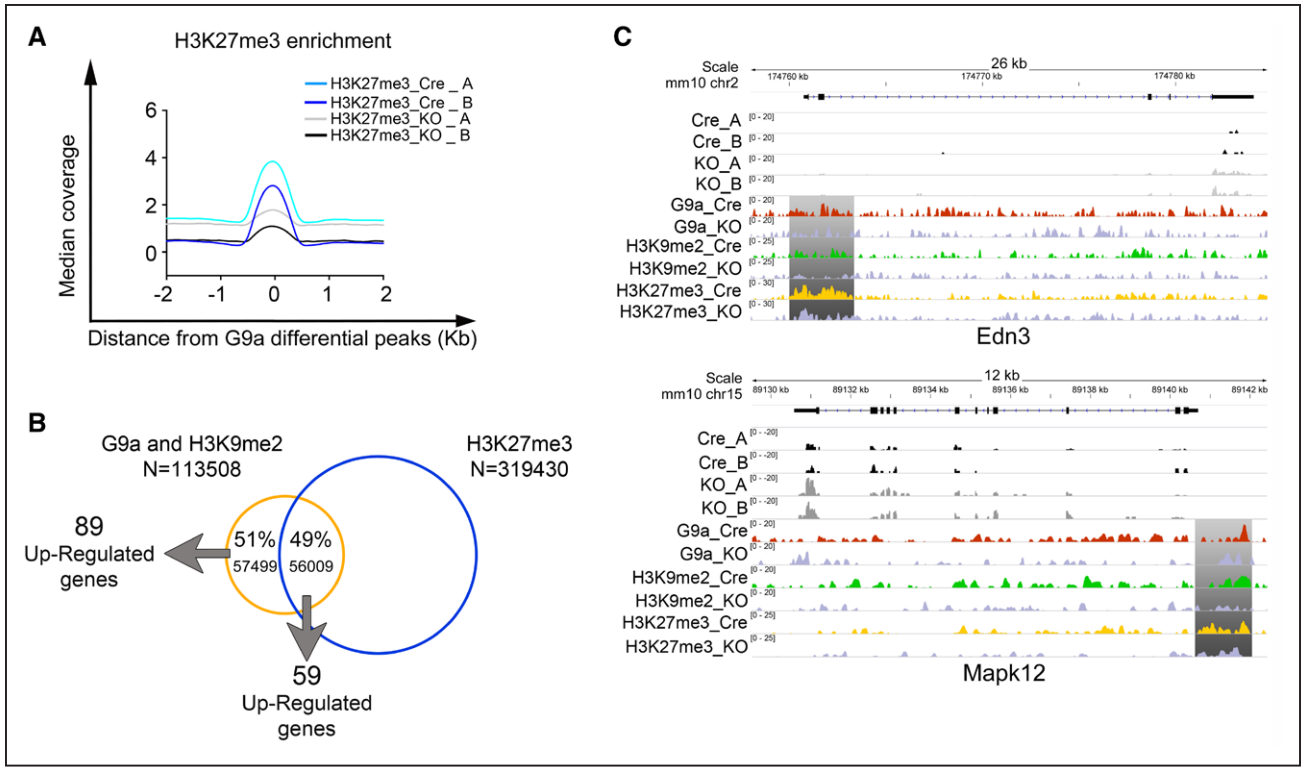

Figure 3. G9a is required for H3K27 trimethylation at a subset of G9a target genes.
A, Analysis of the distribution of H3K27me3 ±2 kilobases (kb) from the genomic regions bound to G9a. The genome-wide distribution of H3K27me3 was analyzed by chromatin immunoprecipitation sequencing (ChIP-seq) in Cre vs G9a knockout (KO) cardiomyocytes. The G9a-bound genomic regions were identified, comparing ChIP-seq for G9a in Cre vs G9a-KO cardiomyocytes. **B**, Venn diagram of the overlap between the best G9a-bound genomic regions (genomic regions losing G9a and H3K9me2 in G9a-KO cardiomyocytes) and regions with a decreased level of H3K27me3 in G9a-KO cardiomyocytes (H3K27me3 differential peaks). **Arrows** indicate the number of genes upregulated in G9a-KO cardiomyocytes associated with these genomic regions. **C**, RNA sequencing and ChIP-seq profiles for G9a, H3K9me2, and H3K27me3 carried out on Cre and G9a-KO cardiomyocytes on the genes encoding endothelin 3 (*Edn3*) and mitogen-activated protein kinase 12 (*Mapk12*). The distributions of reads for G9a, H3K9me2, and H3K27me3 were obtained from the average distribution of the reads in replicates normalized to input and library dimension.

in the mouse HL-1 cell line. Coimmunoprecipitation assay revealed that there was an interaction between G9a and EZH2 in these cells (Figure IIIA in the online-only Data Supplement).

Next, we evaluated whether loss of G9a had an effect on the distribution of H3K27me3, performing ChIP-seq for H3K27me3 on CMs from Cre and G9a-KO mice. Distribution analysis of H3K27me3 around the G9a peaks revealed that there was a global reduction of H3K27me3 at the G9a-bound genomic regions in G9a-KO CMs (Figure 3A). Clustering analysis (based on the genomic distribution of the ChIP-seq signal) revealed moderate correlation for H3K27me3 (Pearson correlation: 0.50, 0.42, 0.40, and 0.38 for all comparisons between replicates) in Cre CMs versus G9a-KO CMs (Figure IIB in the online-only Data Supplement), indicating that depletion of G9a has a slight impact on the global distribution of the histone mark. By analyzing the overlap of peaks, we found that 49% of the best G9a-bound genomic regions were associated with a downregulated H3K27me3 profile, suggesting that the HMT activity of G9a is required for H3K27 trimethylation at a large subset of targets (Figure 3B). We found 59 upregulated genes associated with these peaks in G9a-KO CMs (Table III in the online-only Data Supplement). Comparative canonical pathways analysis showed that some terms, including glucose, glucose 1-phosphate, and guanosine 5'-diphosphate–glucose biosynthesis degradation, were specific for this data set, indicating that H3K27 trimethylation contributes to the repressive activity of G9a at a specific functional class of gene (Figure IIIB in the online-only Data Supplement). ChIP-seq and RNA-seq distribution reads on the loci encoding endothelin 3 (*Edn3*) and mitogen-activated protein kinase 12 (*Mapk12*) are given in Figure 3C.

G9a Contributes to the Transcription-Repressing Activity of MEF2C in Normal CMs

G9a is unable to bind directly to DNA. Thus, it is conceivable that CM-specific activity of G9a is mediated by interaction with cardiac-specific transcription fac-

tors. G9a has recently been reported to interact with MEF2C during myogenesis, regulating its activity.[26] This finding, together with the key role of MEF2C in regulating cardiac homeostasis and in driving the gene expression changes occurring in cardiac hypertrophy,[3,27,28] led us to investigate whether MEF2C interacts with G9a in CMs and any functional consequences of this. We first performed an endogenous coimmunoprecipitation assay, finding that G9a coimmunoprecipitates with MEF2C in Cre CMs but not in G9a-KO CMs, as expected (Figure 4A). We then tested whether G9a interfered with the transcriptional activity of MEF2C, performing a transcription assay on HEK293 cells transfected with a construct encoding luciferase under the control of the cardiac-specific *NPPA* promoter. Overexpression of MEF2C activated the *NPPA* promoter, as reported previously,[29] whereas overexpression of G9a repressed its activity to an extent similar to histone deacetylase 4 (Figure 4B), a known transcriptional repressor of MEF2.[30]

To further elucidate the function of the G9a-MEF2C interaction in adult CMs, we used ChIP-seq to define the genomic distribution of MEF2C in Cre and G9a-KO CMs, comparing the data sets with those described above. Distribution analysis revealed enrichment in Cre CMs of MEF2C around the G9a peaks that were lost in G9a-KO CMs (Figure 4C). Moreover, there was strong correlation between the genomic distribution of MEF2C and the G9a-bound genomic regions in Cre CMs (Pearson correlation: 0.89, 0.86, 0.83, and 0.82 for all comparisons between replicates). This value was low for MEF2C in Cre CMs versus G9a-KO CMs (Pearson correlation: 0.21, 0.14, 0.14, and 0.12 for all comparisons between replicates; Figure 4D). Thus, G9a and MEF2C colocalize at many genomic regions in vivo, and loss of G9a compromises binding of MEF2C at these loci.

To better identify the genomic regions with cobound MEF2C and G9a, we studied the data set of 329 600 regions with significantly impaired binding (adjusted $P \leq 0.01$) of MEF2C in G9a-KO CMs. A genomic feature association analysis indicated that there was preferential binding of MEF2C to long interspersed nuclear elements and to CpG regions, suggestive of a role for MEF2C in regulating their activities (Figure IVA in the online-only Data Supplement). Next, we cross-compared this data set with that of the best G9a-bound genomic regions, identifying 47 417 regions binding to G9a and to MEF2C. These regions were associated in G9a-KO CMs with 113 modulated genes, 83 of which were upregulated. This set was enriched in genes encoding contractility proteins (eg, nebulette [*NEBL*], *NEB*, myomesin 2 [*MYOM2*], and sorbin and SH3 domain containing 2 [*SORBS2*]). Notably, 56.6% of these genes showed a loss of H3K27me3 (Figure IVB in the online-only Data Supplement), suggesting that PRC2 cooperates with the G9a-MEF2C complex in gene silencing. This was supported by the aforementioned finding of interaction between MEF2C and EZH2 in HL-1 cells (Figure IIIA in the online-only Data Supplement). ChIP-seq and transcriptomic profiles of 2 genes identified as G9a-MEF2C targets are given in Figure 4E.

G9a-MEF2C Is Required for Heterochromatin Maintenance

To determine the chromatin context in which G9a binds to MEF2C, we first defined the chromatin state of the heart, analyzing a set of several Encode Project's ChIP-seq data sets with ChromHMM.[31] In agreement with previously reported data,[32] we identified 15 states: 10 were represented by euchromatic regions (states 1–10) and 5 by repressed chromatin regions, including repressed chromatin (state 11), heterochromatin (states 12–14), and insulators (state 15). When we analyzed how the G9a-MEF2C–bound genomic regions were distributed among the various chromatin states, we found that enrichment of the complex on heterochromatin (67.5% present in states 12–14) was greater than that observed for all MEF2C-bound genomic regions (Figure 5A, left); in addition, the pattern was specific for the heart (Figure 5A, right).

Regions of heterochromatin are gene-poor areas able to silence nearby genes through the spreading of heterochromatic structure from newly adjacent heterochromatin, a phenomenon called position-effect variegation.[33] We thus assessed whether position-effect variegation was compromised in G9a-KO CMs by assessing transcriptional levels at G9a-MEF2C–bound heterochromatin. We found that genes mapping to within 500 kilobases of this heterochromatin were upregulated in G9a-KO CMs, an effect not observed for heterochromatic or euchromatic regions not bound to G9a (Figure 5B and Figure VA in the online-only Data Supplement).

A parameter of heterochromatin organization is the solubility of heterochromatin protein 1 family members (HP1β, HP1β, and HP1γ) from these genomic regions; an increase in solubility is an index of heterochromatin deconstruction.[34] Thus, we assessed the binding of HP1 members to heterochromatin in HL-1 cells on short interfering RNA knockdown of MEF2C and in HL-1 cells treated with the G9a inhibitor BIX-01294. Cells were washed with CSK buffer plus 0.5% Triton-X, a buffer that solubilizes proteins weakly bound to chromatin, and then processed for Western blotting. We found that depletion of MEF2C and inhibition of G9a increased the solubility of HP1β and HP1γ, whereas they had no effect on HP1α, a marker of centromeric heterochromatin (Figure 5C). Thus, the G9a-MEF2C complex is required for maintaining the correct structure of noncentromeric heterochromatin.

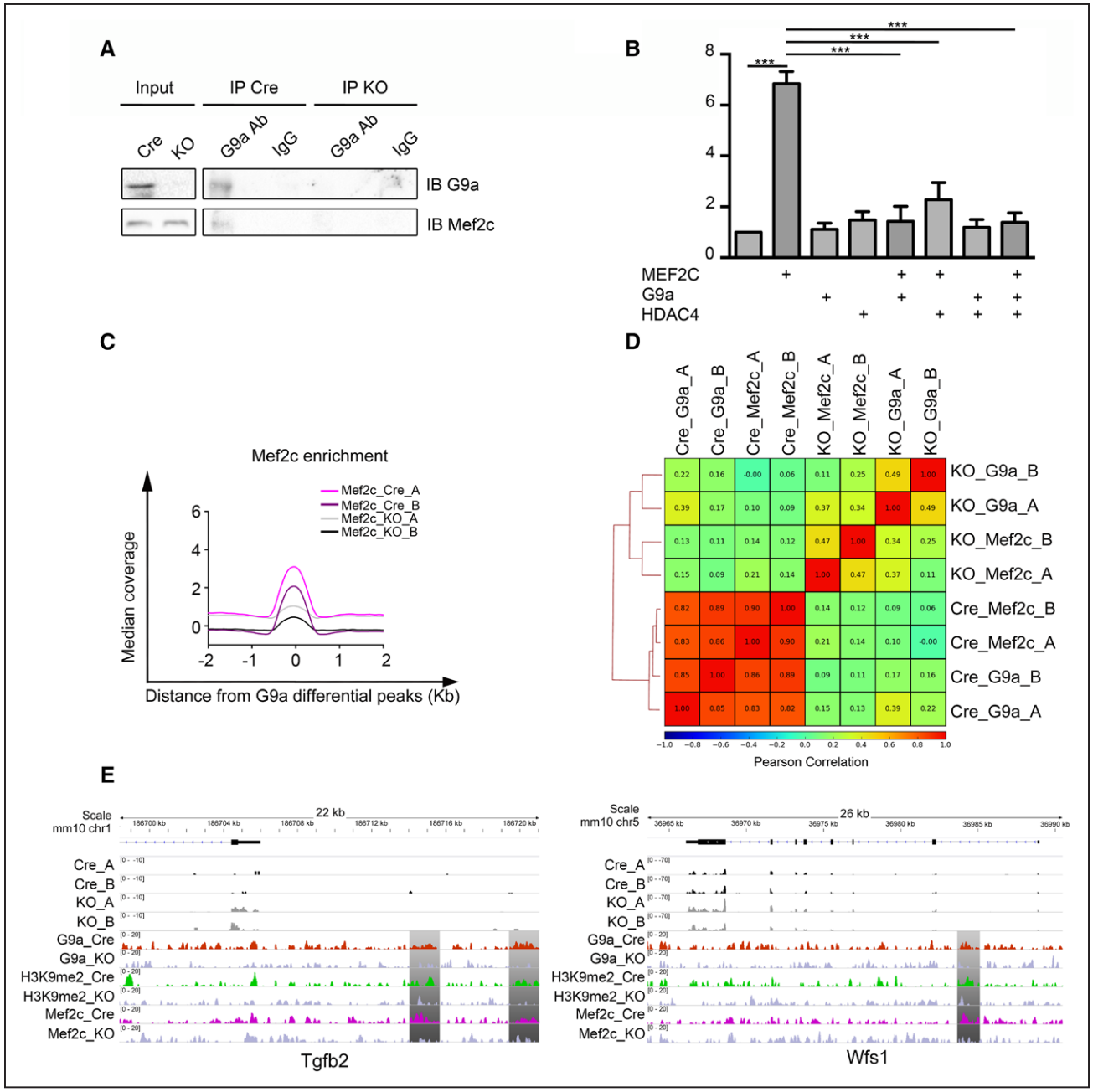

Figure 4. G9a binds to and represses the transcriptional activity of MEF2C in normal cardiomyocytes.
A, Whole extracts of cardiomyocytes purified from G9a knockout (KO) and Cre mice were immunoprecipitated (IP) with an antibody against G9a and then blotted with antibodies against G9a (**top**) and MEF2C (**bottom**). **B**, Luciferase assay using the cardiac-specific, MEF2C-responsive atrial natriuretic peptide (*Nppa*) promoter. HEK293 cells were transfected with the ANF-luc reporter and MEF2C, G9A, or histone deacetylase 4 (HDAC4) as indicated. Lysates were processed for Renilla and Firefly luciferase emission and plotted as indicated. ***$P<0.001$. **C**, Analysis of distribution of MEF2C ±2 kilobases (kb) from the best G9a-bound genomic regions. The genome-wide distribution of MEF2C was analyzed by chromatin immunoprecipitation sequencing (ChIP-seq) in Cre vs G9a-KO cardiomyocytes. **D**, Clustered heat map of pair-wise Pearson correlation of the distributions of MEF2C and G9a in Cre and G9a-KO cardiomyocyte genomes. **E**, RNA sequencing and ChIP-seq profiles for G9a, H3K9me2, and MEF2C on transforming growth factor beta 2 (*Tgfb2*) and Wolframin ER transmembrane glycoprotein (*Wfs1*) in Cre and G9a-KO cardiomyocytes. The distributions of reads for G9a, H3K9me2, and MEF2C were obtained from the average distribution of replicates normalized to input and library dimension.

To address the role of G9a-MEF2C–dependent facultative heterochromatin, we looked for significantly modulated genes mapping within 200 kilobases from these heterochromatin regions in G9a-KO CMs, excluding those genes that had the G9a-MEF2C complex bound ±10 kilobases from the transcription start site. Gene

A

	all Mef2c	G9a/Mef2c
1_Txn_Elongation	7.6%	2.1%
2_Weak_Txn	18.0%	7.8%
3_Txn_Transition	10.1%	4.5%
4_Poised_Enhancer	2.2%	0.8%
5_Active_Promoter	1.2%	0.6%
6_Strong_Enhancer	0.5%	0.2%
7_Active_Promoter	1.8%	0.5%
8_Strong_Enhancer	1.1%	0.8%
9_Strong_Enhancer	7.2%	5.5%
10_Poised_Promoter	1.3%	0.9%
11_Repressed	6.2%	8.0%
12_Heterochrom	16.9%	34.5%
13_Heterochrom	7.5%	18.4%
14_Heterochrom	17.1%	14.6%
15_Insulator	1.3%	0.7%

	% heart	% brain	% intestine	% kidney	% liver	% spleen	% testes	% thymus	% mESC
1_Txn_Elongation	2.1%	3.6%	3.5%	3.4%	3.4%	4.8%	3.6%	2.6%	2.8%
2_Weak_Txn	7.8%	4.7%	4.3%	6.8%	3.4%	6.6%	4.7%	3.4%	5.6%
3_Txn_Transition	4.5%	1.4%	1.0%	1.0%	0.8%	0.5%	0.8%	0.8%	0.9%
4_Poised_Enhancer	0.8%	0.1%	0.1%	0.1%	0.1%	0.1%	0.6%	0.1%	0.2%
5_Active_Promoter	0.6%	0.1%	0.6%	0.5%	0.1%	0.5%	4.4%	0.1%	1.8%
6_Strong_Enhancer	0.2%	0.8%	0.6%	0.3%	0.5%	0.1%	1.4%	0.6%	0.3%
7_Active_Promoter	0.5%	0.0%	0.5%	0.6%	0.2%	0.5%	0.5%	0.2%	0.6%
8_Strong_Enhancer	0.8%	3.9%	2.8%	3.8%	2.8%	2.3%	1.0%	2.9%	1.9%
9_Strong_Enhancer	5.5%	14.4%	7.4%	5.9%	5.1%	2.1%	5.9%	5.2%	6.3%
10_Poised_Promoter	0.9%	1.2%	0.7%	0.6%	0.4%	0.6%	1.3%	0.4%	1.3%
11_Repressed	8.0%	1.9%	2.6%	4.2%	1.2%	3.5%	1.1%	1.2%	9.7%
12_Heterochrom	34.5%	1.3%	5.1%	38.4%	1.3%	38.5%	1.5%	1.3%	52.1%
13_Heterochrom	18.4%	10.8%	14.5%	17.2%	14.2%	29.6%	13.9%	14.3%	6.6%
14_Heterochrom	14.6%	53.2%	48.2%	15.8%	54.7%	9.9%	50.8%	55.2%	9.1%
15_Insulator	0.7%	2.6%	8.0%	1.3%	11.6%	0.4%	8.6%	11.7%	0.8%

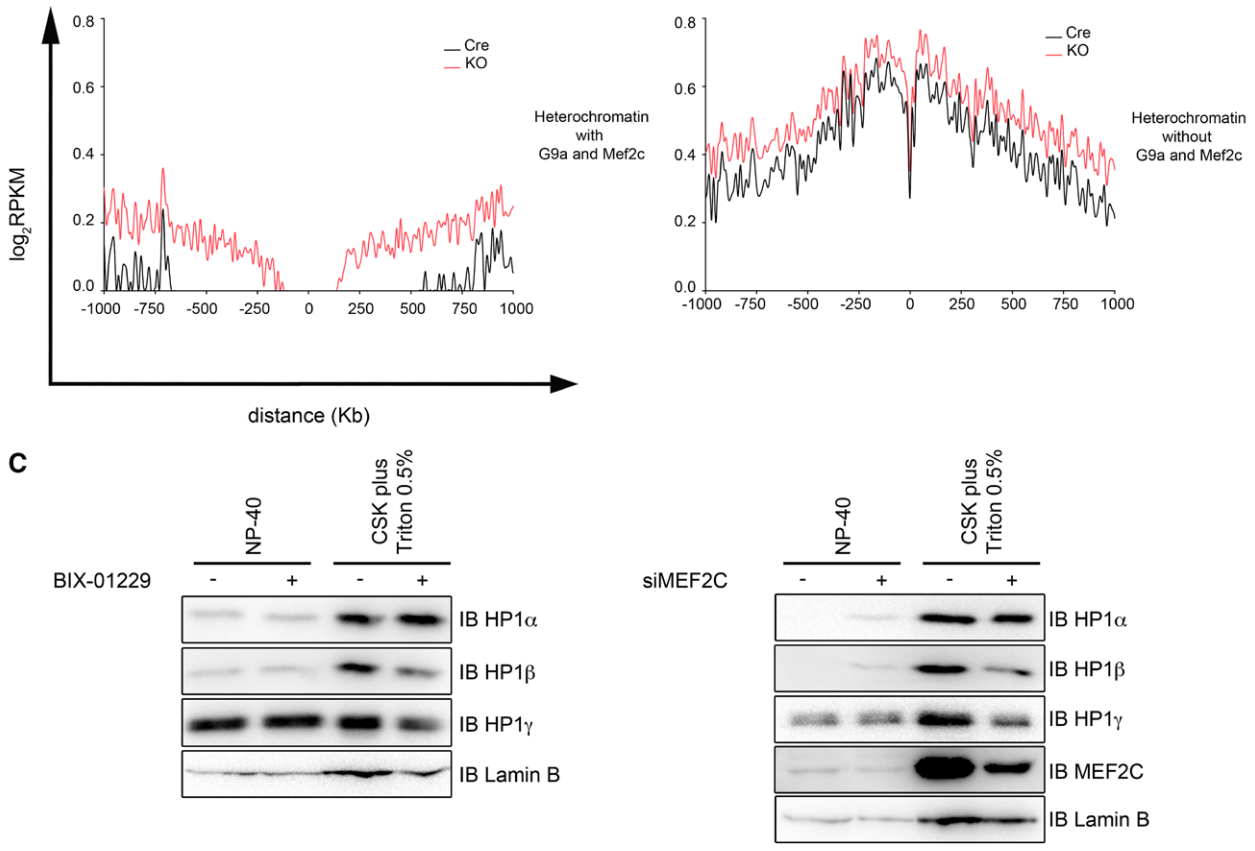

Figure 5. The G9a-MEF2C complex binds heterochromatin and is required for its silencing.
A, Percentages of genomic regions binding the G9a-MEF2C complex mapping to the various states of chromatin. **Left** table compares the genomic distribution of the G9a-MEF2C complex with that of MEF2C in heart; **right** table gives the distribution of the G9a-MEF2C complex in heart and other tissues. Colors indicate different chromatin states. **B**, The level of transcription around regions of heterochromatin bound to G9a-MEF2C in Cre and G9a knockout (KO) cardiomyocytes (**left**). As a control, we analyzed transcriptional levels around heterochromatin regions not bound to G9a-MEF2C (**right**). The curves are calculated with cubic spline regression. **C**, HL-1 cells treated with 8 μmol/L of the G9a inhibitor BIX-01294 for 48 hours (**left**) and HL-1 cells in which MEF2C was knocked down (**right**) were washed with CSK buffer plus 0.5% Triton X-100. Lysates were analyzed by Western blotting with the indicated antibodies. HP1 indicates heterochromatin protein 1 family members; IB, immunoblot; kb, kilobases; mESC, mouse embryonic stem cells; and RPKM, reads per kilobases per million.

Ontology identified 33 upregulated genes involved in heart development such as BHLH transcription factor 1 (*Hes1*), ankyrin repeat domain 1 (*Ankrd1*), and xin actin-binding repeat-containing 2 (*Xirp2*; Figure VB and VC in the online-only Data Supplement). ChIP analysis of these heterochromatic regions revealed that on MEF2C silencing in HL-1 cells, the enrichment of H3K9me2 and H3K27me3 decreased, confirming that MEF2C is required for the deposition of G9a-dependent methylation marks (Figure VB in the online-only Data Supplement).

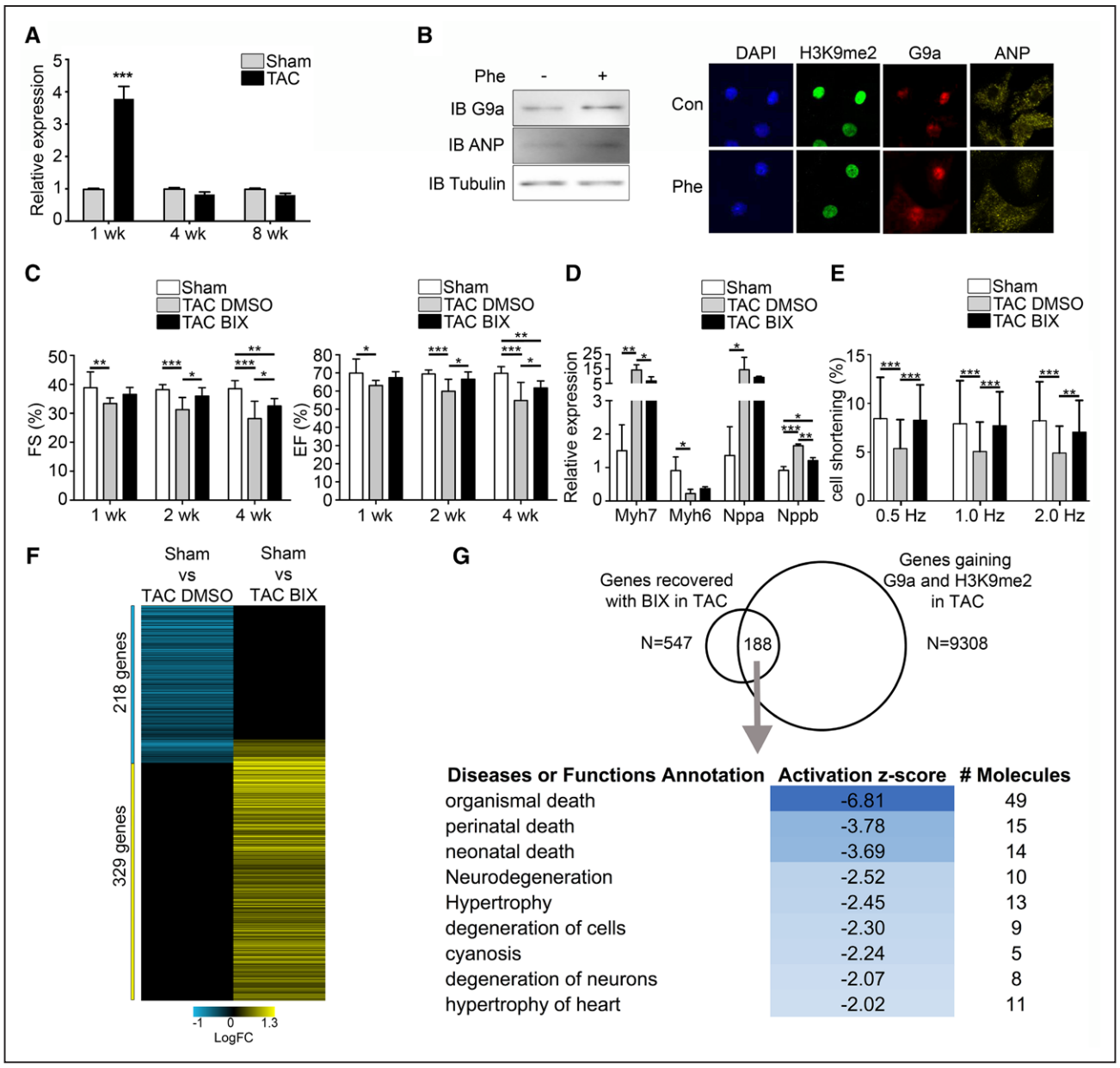

Diseases or Functions Annotation	Activation z-score	# Molecules
organismal death	-6.81	49
perinatal death	-3.78	15
neonatal death	-3.69	14
Neurodegeneration	-2.52	10
Hypertrophy	-2.45	13
degeneration of cells	-2.30	9
cyanosis	-2.24	5
degeneration of neurons	-2.07	8
hypertrophy of heart	-2.02	11

Figure 6. G9a promotes cardiac hypertrophy by repressing expression of a large set of antihypertrophic genes. **A**, Quantitative real-time polymerase chain reaction analyses of *G9a* expression in whole left ventricular tissue of mice subjected to transverse aortic constriction (TAC) for 1, 4, and 8 weeks (mean±SD; n=3). Glyceraldehyde 3-phosphate dehydrogenase (*Gapdh*) was used as a housekeeping gene. **B**, Representative Western blot for G9a in total extracts of neonatal mouse cardiomyocytes treated for 6 hours with 100 μm phenylephrine; tubulin was used as a control (**left**). Immunostaining for H3K9me2, G9a, and atrial natriuretic peptide (ANP) on neonatal mouse cardiomyocytes treated for 6 hours with 100 μm phenylephrine (Phe) (**right**). Perinuclear localization of ANP in Phe-treated cardiomyocytes is consistent with induction of hypertrophy. **C**, Percent fractional shortening (FS) and ejection fraction (EF) in mice subjected to TAC for 1, 2, and 4 weeks and treated with 20 mg/mL of the G9a inhibitor BIX-01294 by infusion. As a control, we used mice treated with dimethyl sulfoxide (DMSO; n=10 mice for each group). **D**, Quantitative real-time polymerase chain reaction analysis of mRNA levels of the hypertrophic markers fetal myosin heavy chain (*Myh7*), adult myosin heavy chain (*Myh6*), atrial natriuretic peptide (*Nppa*), and brain natriuretic peptide (*Nppb*) in whole left ventricular tissue (mean±SD; n=3) of mice subjected to TAC for 1 week and treated with the G9a inhibitor BIX-01294. As a control we used mice treated with DMSO. **E**, Contractility in cardiomyocytes isolated from the heart of mice subjected to TAC for 1 week and treated with the G9a inhibitor BIX-01294 (n=49–64 cardiomyocytes). **F**, Heat map of log fold-change (logFC) values for 547 genes with expressions that were restored (cluster A, 218 genes) or increased (cluster B, 329 genes) after treatment with BIX-01294 in cardiomyocytes isolated from mice subjected to TAC for 1 week. Differential gene expression analysis was carried out with Illumina gene expression array. The unmodulated and the not significantly modulated (adjusted *P*>0.1) genes are shown in black. **G**, Venn diagram of the overlap between the 547 genes described above with (*Continued*)

G9a Represses the Expression of Antihypertrophic Genes in CMs of Pressure-Overloaded Mice

The function of G9a in HF is controversial. One study has reported that cardiac G9a expression is increased in mice subjected to TAC for 1 week and that the activity of this HMT is required for cardiac hypertrophy in vivo[21]; in contrast, a more recent study found that G9a is downregulated after 6 weeks of TAC and provided evidence of an antihypertrophic activity for this HMT in vitro.[22] These conflicting results could be due to the different time points analyzed in the 2 studies. To address this point, we assessed G9a expression in the left ventricle of mice after 1, 4, and 8 weeks of TAC. We found G9a upregulated at 1 week but not at the later time points (Figure 6A). Supporting this, G9a was upregulated in neonatal mouse CMs treated in vitro for 6 hours with phenylephrine, an α-1 receptor agonist that induces hypertrophic growth (Figure 6B). Thus, G9a is upregulated during the initial stages of cardiac hypertrophy, supporting the notion of an antihypertrophic activity for this HMT in the early phase of the disease. In agreement, administration of BIX-01294 to TAC mice improved cardiac function and inhibited the development of hypertrophy, as shown by echocardiographic data and mRNA levels of the hypertrophic markers *Myh7*, *Nppa*, and *Nppb* (Figure 6C and 6D); moreover, contractility was improved (Figure 6E). Coherently with the phenotype of G9a KO mice at baseline, sham mice treated with the G9a inhibitor had decreased heart function (Figure VIA in the online-only Data Supplement). The effect of G9a inhibition on cardiac hypertrophy was not investigated with the KO mice model because of the technical inability of inducing G9a KO in concomitance with pressure overload and a baseline decrease in cardiac function induced by deleting G9a in CMs.

To address how G9a promotes cardiac hypertrophy, we assessed the gene expression signature defined by G9a in TAC CMs. To this end, we compared the expression profiles of CMs isolated from BIX-01294–treated mice and control groups (untreated and dimethyl sulfoxide–treated mice at baseline and after TAC). Chemical inhibition of G9a modulated the expression of 547 genes after TAC (Table IV in the online-only Data Supplement). Because G9a is a transcriptional repressor, we focused our attention on the upregulated genes, which included those with an expression that was either restored (cluster A, 218 genes) or increased (cluster B, 329 genes) after drug treatment (Figure 6F). To determine potential direct targets of G9a, we identified which of these genes acquired G9a binding in TAC CMs. To this end, we identified the best G9a-bound genomic regions acquired in hypertrophic CMs as those that had a significant increase in the levels of both G9a and H3K9me2. These regions were identified by comparing the genome-wide distributions of G9a and H3K9me2 (as defined by ChIP-seq) in CMs isolated from TAC mice at 1 week with those from sham mice. The Genomic Regions Enrichment of Annotations Tool[35] identified 21 708 best G9a-bound genomic regions specific to hypertrophic CMs that mapped to the regulatory regions of 9308 genes (Figure 6G).

By crossing microarray results with our data set of best G9a-bound genomic regions, we found that of the 547 genes with an expression that was restored in TAC mice after treatment with BIX-01294, 188 acquired binding to G9a (Figure 6G). Ingenuity Pathway Analysis revealed that these genes were involved in disease processes strongly correlated with cardiac hypertrophy (eg, organismal death, myocardial dysfunction, and cell degeneration) but had negative *z* scores, indicating that they are negative regulators of those pathways (Figure 6G and Table V in the online-only Data Supplement). Genes encoding contractile apparatus proteins such as myosin light chain kinase 3 and desmin and genes encoding vascular endothelial growth factor were among those repressed by G9a in TAC mice.

The foregoing results indicate that G9a cooperates with PRC2 in maintaining gene silencing in the normal heart through the promotion of trimethylation at H3K27. To see if this occurs also during cardiac hypertrophy, we examined the distribution of H3K27me3 on genomic regions acquiring G9a in TAC CMs. ChIP-seq for H3K27me3 showed that 117 genes repressed by G9a in TAC CMs acquired the mark (Table V in the online-only Data Supplement). These genes were enriched in pathways negatively regulating hypertrophy and organismal death; genes that lost the mark were implicated in cell degeneration and lipid concentration (Figure VIB in the online-only Data Supplement).

Thus, G9a promotes cardiac hypertrophy by repressing a set of antihypertrophic genes via H3K9me2 deposition, and similar to what we observed in normal heart, G9a cooperates with PRC2 in the silencing of a subset of its target genes.

DISCUSSION

Correct gene expression in CMs is fundamental for the normal functioning of the heart.[36] The role of histone

Figure 6 Continued. 9308 genes associated with genomic regions that acquired G9a binding in cardiomyocytes purified from 1-week TAC mice (**top**). Table of Ingenuity Pathway Analysis disease and function analysis of the 188 genes resulting from the overlap of the 2 data sets. The repressed pathways are in blue (*z* score <0; **bottom**). BIX indicates BIX-01229; DAPI, 4',6-diamidin-2-fenilindolo; and IB, immunoblot. **P*<0.05. ***P*<0.01. ****P*<0.001.

methyltransferases such as EZH2 and DOT1L in establishing the transcriptional program of postnatal CMs during heart development has been shown.[37,38] However, the function of this class of epigenetic enzymes is still largely unexplored for postnatal heart physiology and disease. Here, we show that the HMT G9a is necessary for correct gene expression in normal CMs and for driving the changes in gene expression underlying cardiac hypertrophy. This dual function is linked to the ability of G9a to repress, through dimethylation of lysine 9 at histone H3, different classes of genes, depending on the functional status of the heart. We also found a synergy between G9a and EZH2, the catalytic subunit of PRC2, in the silencing of genes, so EZH2 seems important for the maintenance of homeostasis in postmitotic CMs and for correct differentiation of cardiac progenitor cells.[37]

Among genes repressed by G9a were genes encoding proteins involved in calcium signaling and contractility. One in particular was myosin binding protein C, a member of a gene family found mutated in ≈30% of patients with hypertrophic cardiomyopathy.[39] It could therefore be conjectured that at least part of the significant phenotypic heterogeneity seen even within a given mutation of this gene may be due to defects in the epigenetic modulation of its expression.

A general question concerning epigenetic enzymes is whether and how they exert cell type–specific activity. Our results suggest that this may take place in CMs through the interaction with transcription factors such as MEF2C, which plays a key role in heart homeostasis and hypertrophy.[3,27,28] As a matter of fact, MEF2C and G9a colocalize at many genomic regions (42% of G9a-bound genomic regions also bind MEF2C). Our results also identify H3K9me2 as a new epigenetic mark for MEF2C-driven repression in the unstressed heart. Consistent with this finding, decreased dimethylation and trimethylation of H3K9 at the promoter regions of atrial natriuretic peptide and brain natriuretic peptide genes, both of which are targeted by MEF2C, have been observed in the myocardium of patients with HF.[40] Our results do not exclude the possibility that further cardiac transcription factors, including other members of the MEF family expressed in heart (MEF2A and MEF2D), could be involved in recruiting G9a to specific genomic sites.

Remarkably, inhibition of G9a in CMs is sufficient to impair cardiac function, unlike the KO of histone deacetylase 5 and 9, which does not produce a cardiac phenotype in the absence of external stress.[3,41,42] These results suggest that dimethylation of H3K9 catalyzed by G9a is dominant over deacetylation in maintaining CM gene expression under physiological conditions.

MEF2 is viewed as a family of transcription factors (MEF2A, MEF2B, MEF2C, and MEF2D) that regulate transcription through binding to regulator elements such as promoters and enhancers.[7,43] In the unstressed heart, we found that MEF2C also binds to heterochromatin as part of a complex with G9a and is required for mediating transcription silencing at these genomic regions. Thus, we propose a model whereby G9a promotes the gene silencing required for heart homeostasis through interaction with MEF2C, determining not only a repressive epigenetic signature on genes but also heterochromatinization. Our findings demonstrating a role for MEF2C in maintaining heterochromatin in adult CMs further the understanding of the molecular mechanisms underlying heterochromatinization in postmitotic cells. Although evidence has previously been provided on the role of G9a in the formation of facultative heterochromatin,[13,14] the mechanisms through which G9a drives these processes are not known yet. Here, we show that in CMs, MEF2C binds genomic regions enriched in long interspersed nuclear elements and CpG islands, 2 genetic elements that trigger the formation of heterochromatin.[44] The finding that the G9a-MEF2C complex regulates regions of heterochromatin responsible for the silencing of some developmental genes via position-effect variegation, together with the known role of MEF2C in regulating gene expression changes occurring in heart development,[43] leads us to speculate that this complex is involved in defining the heterochromatin domain during CM differentiation.

G9a and Hypertrophy

Histone and DNA modifications contribute to creating the epigenetic signature of cardiac hypertrophy.[7,45,46] However, the molecular mechanisms generating this signature are not known. Here, we show that during early cardiac hypertrophy, G9a is needed for the transcriptional repression of genes encoding negative regulators of pathways associated with impairment of CM function through H3K9 dimethylation. Among these, we found the genes encoding cardiac myosin light chain kinase, the repression of which causes sarcomeric disorganization during the transition from compensated to decompensated hypertrophy,[47,48] and vascular endothelial growth factor, a key angiogenic molecule that, when silenced in the stressed heart, causes an impairment of coronary angiogenesis, promoting CM apoptosis.[49,50] Of note, inhibition of G9a increased the expression of the master angiogenic factor hypoxia-inducible factor 1α. G9a also promoted transcriptional repression via interaction with PRC2, suggesting not only that the development of hypertrophy is dependent on the inhibition of PRC2 by the long noncoding RNA Chear, as described elsewhere,[51] but also that the activity of PRC2 is required for gene silencing at a subset of genes regulated by G9a. On the basis of these findings, G9a emerges as a critical player in defining the transcriptional program also during cardiac hypertrophy.

The role of G9a in regulating cardiac hypertrophy has been the subject of recent reports. In 1 study, G9a

was found to be part of a repressive chromatin complex responsible for silencing hypertrophy-induced *Myh6* in stressed heart.[21] In contrast, a more recent report described G9a as prohypertrophic.[22] One possible explanation for these 2 apparently differing results could be the different experimental kinetics of hypertrophy induction. Whereas Han et al[21] focused attention on the role of G9a in early hypertrophy (1 week of TAC), Thienpont et al[22] analyzed a later time point (6 weeks of TAC). It is therefore tempting to speculate that the function of G9a is dependent on the stage of hypertrophy development. In the unstressed heart, G9a is required for correct gene transcription and thus cardiac function, whereas on stress, it is first required for inducing cardiac hypertrophy but later plays an antihypertrophic role.

Our data suggest that G9a represents a potential target for the treatment of early-stage cardiac hypertrophy. However, evidence of the dual role played by G9a, not only in healthy versus diseased hearts but also in different stages of HF progression, hampers the use of direct inhibitors of G9a as a safe therapeutic tool. Nonetheless, it is possible to envision the development of molecules that affect the function of G9a during the early phase of hypertrophy. Future studies will provide a deeper understanding of the mechanism of action of G9a. Indeed, identification of the transcription factors that recruit G9a to cardiac-specific genes at the onset of disease could enable the design of pharmacological tools that prevent these interactions.

ACKNOWLEDGEMENTS

We thank Alexander Tarakhovsky (Rockefeller University) for providing the *G9a*$^{f/f}$ mice.

SOURCES OF FUNDING

This research was supported by a European Research Council (ERC) Advanced Grant (CardioEpigen, No. 294609), ERC Proof of Concept grant (No. 713734), the Italian Ministry of Health (PE-2013-02356818), the Cariplo Foundation (2015-0573), and the Italian Ministry of Education, University and Research (2015583WMX) to Dr Condorelli, and the National Research Council of Italy through the project schemes EPIGEN (Flagship Project Epigenomica) and Ageing (Flagship Project Invecchiamento) to Dr Papait. Dr Pagiatakis was supported in part by a Gerry Scotti Fellowship.

DISCLOSURES

None.

AFFILIATIONS

From Department of Cardiovascular Medicine, Humanitas Research Hospital, Rozzano, Milan, Italy (R.P., S.S., C.P., F.R., P.C., N.S., M. Miragoli, G.C.); Genetic and Biomedical Research Institute, National Research Council of Italy, Rozzano, Milan, Italy (R.P., F.R., P.C., N.S., G.C.); Humanitas University, Rozzano, Milan, Italy (M. Mazzola, G.C.); School of Medicine, University of Verona, Italy (M. Mazzola); and Department of Medicine and Surgery, University of Parma, Italy (M. Miragoli).

FOOTNOTES

Received March 31, 2017; accepted July 21, 2017.

The online-only Data Supplement is available with this article at http://circ.ahajournals.org/lookup/suppl/doi:10.1161/CIRCULATIONAHA.117.028561/-/DC1.

Circulation is available at http://circ.ahajournals.org.

REFERENCES

1. McMurray JJ. Clinical practice: systolic heart failure. *N Engl J Med*. 2010;362:228–238. doi: 10.1056/NEJMcp0909392.
2. Lompre AM, Schwartz K, d'Albis A, Lacombe G, Van Thiem N, Swynghedauw B. Myosin isoenzyme redistribution in chronic heart overload. *Nature*. 1979;282:105–107.
3. Zhang CL, McKinsey TA, Chang S, Antos CL, Hill JA, Olson EN. Class II histone deacetylases act as signal-responsive repressors of cardiac hypertrophy. *Cell*. 2002;110:479–488.
4. Greco CM, Condorelli G. Epigenetic modifications and noncoding RNAs in cardiac hypertrophy and failure. *Nat Rev Cardiol*. 2015;12:488–497. doi: 10.1038/nrcardio.2015.71.
5. Greer EL, Shi Y. Histone methylation: a dynamic mark in health, disease and inheritance. *Nat Rev Genet*. 2012;13:343–357. doi: 10.1038/nrg3173.
6. Stein AB, Jones TA, Herron TJ, Patel SR, Day SM, Noujaim SF, Milstein ML, Klos M, Furspan PB, Jalife J, Dressler GR. Loss of H3K4 methylation destabilizes gene expression patterns and physiological functions in adult murine cardiomyocytes. *J Clin Invest*. 2011;121:2641–2650. doi: 10.1172/JCI44641.
7. Papait R, Cattaneo P, Kunderfranco P, Greco C, Carullo P, Guffanti A, Viganò V, Stirparo GG, Latronico MV, Hasenfuss G, Chen J, Condorelli G. Genome-wide analysis of histone marks identifying an epigenetic signature of promoters and enhancers underlying cardiac hypertrophy. *Proc Natl Acad Sci USA*. 2013;110:20164–20169. doi: 10.1073/pnas.1315155110.
8. Zhang QJ, Chen HZ, Wang L, Liu DP, Hill JA, Liu ZP. The histone trimethyllysine demethylase JMJD2A promotes cardiac hypertrophy in response to hypertrophic stimuli in mice. *J Clin Invest*. 2011;121:2447–2456. doi: 10.1172/JCI46277.
9. Antignano F, Burrows K, Hughes MR, Han JM, Kron KJ, Penrod NM, Oudhoff MJ, Wang SK, Min PH, Gold MJ, Chenery AL, Braam MJ, Fung TC, Rossi FM, McNagny KM, Arrowsmith CH, Lupien M, Levings MK, Zaph C. Methyltransferase G9A regulates T cell differentiation during murine intestinal inflammation. *J Clin Invest*. 2014;124:1945–1955. doi: 10.1172/JCI69592.
10. Shinkai Y, Tachibana M. H3K9 methyltransferase G9a and the related molecule GLP. *Genes Dev*. 2011;25:781–788. doi: 10.1101/gad.2027411.
11. Tachibana M, Ueda J, Fukuda M, Takeda N, Ohta T, Iwanari H, Sakihama T, Kodama T, Hamakubo T, Shinkai Y. Histone methyltransferases G9a and GLP form heteromeric complexes and are both crucial for methylation of euchromatin at H3-K9. *Genes Dev*. 2005;19:815–826. doi: 10.1101/gad.1284005.
12. Tachibana M, Matsumura Y, Fukuda M, Kimura H, Shinkai Y. G9a/GLP complexes independently mediate H3K9 and DNA methylation to silence transcription. *EMBO J*. 2008;27:2681–2690. doi: 10.1038/emboj.2008.192.
13. Lyons DB, Magklara A, Goh T, Sampath SC, Schaefer A, Schotta G, Lomvardas S. Heterochromatin-mediated gene silencing facilitates the diversification of olfactory neurons. *Cell Rep*. 2014;9:884–892. doi: 10.1016/j.celrep.2014.10.001.
14. Pandey RR, Mondal T, Mohammad F, Enroth S, Redrup L, Komorowski J, Nagano T, Mancini-Dinardo D, Kanduri C. Kcnq1ot1 antisense noncoding RNA mediates lineage-specific transcriptional silencing through chromatin-level regulation. *Mol Cell*. 2008;32:232–246. doi: 10.1016/j.molcel.2008.08.022.
15. Mozzetta C, Pontis J, Fritsch L, Robin P, Portoso M, Proux C, Margueron R, Ait-Si-Ali S. The histone H3 lysine 9 methyltransferases G9a and GLP regulate polycomb repressive complex 2-mediated gene silencing. *Mol Cell*. 2014;53:277–289. doi: 10.1016/j.molcel.2013.12.005.

16. Zylicz JJ, Dietmann S, Gunesdogan U, Hackett JA, Cougot D, Lee C, Surani MA. Chromatin dynamics and the role of g9a in gene regulation and enhancer silencing during early mouse development. *Elife*. 2015;4:e09571. doi: 10.7554/eLife.09571.
17. Tachibana M, Sugimoto K, Nozaki M, Ueda J, Ohta T, Ohki M, Fukuda M, Takeda N, Niida H, Kato H, Shinkai Y. G9a histone methyltransferase plays a dominant role in euchromatic histone H3 lysine 9 methylation and is essential for early embryogenesis. *Genes Dev*. 2002;16:1779–1791. doi: 10.1101/gad.989402.
18. Feldman N, Gerson A, Fang J, Li E, Zhang Y, Shinkai Y, Cedar H, Bergman Y. G9a-mediated irreversible epigenetic inactivation of Oct-3/4 during early embryogenesis. *Nat Cell Biol*. 2006;8:188–194. doi: 10.1038/ncb1353.
19. Schaefer A, Sampath SC, Intrator A, Min A, Gertler TS, Surmeier DJ, Tarakhovsky A, Greengard P. Control of cognition and adaptive behavior by the GLP/G9a epigenetic suppressor complex. *Neuron*. 2009;64:678–691. doi: 10.1016/j.neuron.2009.11.019.
20. Casciello F, Windloch K, Gannon F, Lee JS. Functional role of G9a histone methyltransferase in cancer. *Front Immunol*. 2015;6:487. doi: 10.3389/fimmu.2015.00487.
21. Han P, Li W, Yang J, Shang C, Lin CH, Cheng W, Hang CT, Cheng HL, Chen CH, Wong J, Xiong Y, Zhao M, Drakos SG, Ghetti A, Li DY, Bernstein D, Chen HS, Quertermous T, Chang CP. Epigenetic response to environmental stress: assembly of BRG1-G9a/GLP-DNMT3 repressive chromatin complex on Myh6 promoter in pathologically stressed hearts. *Biochim Biophys Acta*. 2016;1863(pt B):1772–1781. doi: 10.1016/j.bbamcr.2016.03.002.
22. Thienpont B, Aronsen JM, Robinson EL, Okkenhaug H, Loche E, Ferrini A, Brien P, Alkass K, Tomasso A, Agrawal A, Bergmann O, Sjaastad I, Reik W, Roderick HL. The H3K9 dimethyltransferases EHMT1/2 protect against pathological cardiac hypertrophy. *J Clin Invest*. 2017;127:335–348. doi: 10.1172/JCI88353.
23. Rockman HA, Ross RS, Harris AN, Knowlton KU, Steinhelper ME, Field LJ, Ross J Jr, Chien KR. Segregation of atrial-specific and inducible expression of an atrial natriuretic factor transgene in an in vivo murine model of cardiac hypertrophy. *Proc Natl Acad Sci USA*. 1991;88:8277–8281.
24. Savi M, Rossi S, Bocchi L, Gennaccaro L, Cacciani F, Perotti A, Amidani D, Alinovi R, Goldoni M, Aliatis I, Lottici PP, Bersani D, Campanini M, Pinelli S, Petyx M, Frati C, Gervasi A, Urbanek K, Quaini F, Buschini A, Stilli D, Rivetti C, Macchi E, Mutti A, Miragoli M, Zaniboni M. Titanium dioxide nanoparticles promote arrhythmias via a direct interaction with rat cardiac tissue. *Part Fibre Toxicol*. 2014;11:63. doi: 10.1186/s12989-014-0063-3.
25. Rusconi F, Ceriotti P, Miragoli M, Carullo P, Salvarani N, Rocchetti M, Di Pasquale E, Rossi S, Tessari M, Caprari S, Cazade M, Kunderfranco P, Chemin J, Bang ML, Polticelli F, Zaza A, Faggian G, Condorelli G, Catalucci D. Peptidomimetic targeting of Cavβ2 overcomes dysregulation of the L-type calcium channel density and recovers cardiac function. *Circulation*. 2016;134:534–546. doi: 10.1161/CIRCULATIONAHA.116.021347.
26. Ow JR, Palanichamy Kala M, Rao VK, Choi MH, Bharathy N, Taneja R. G9a inhibits MEF2C activity to control sarcomere assembly. *Sci Rep*. 2016;6:34163. doi: 10.1038/srep34163.
27. Xu J, Gong NL, Bodi I, Aronow BJ, Backx PH, Molkentin JD. Myocyte enhancer factors 2a and 2c induce dilated cardiomyopathy in transgenic mice. *J Biol Chem*. 2006;281:9152–9162. doi: 10.1074/jbc.M510217200.
28. Kolodziejczyk SM, Wang L, Balazsi K, DeRepentigny Y, Kothary R, Megeney LA. MEF2 is upregulated during cardiac hypertrophy and is required for normal post-natal growth of the myocardium. *Curr Biol*. 1999;9:1203–1206. doi: 10.1016/S0960-9822(00)80027-5.
29. Zang MX, Li Y, Xue LX, Jia HT, Jing H. Cooperative activation of atrial naturetic peptide promoter by dHAND and MEF2C. *J Cell Biochem*. 2004;93:1255–1266. doi: 10.1002/jcb.20225.
30. Miska EA, Karlsson C, Langley E, Nielsen SJ, Pines J, Kouzarides T. HDAC4 deacetylase associates with and represses the MEF2 transcription factor. *EMBO J*. 1999;18:5099–5107. doi: 10.1093/emboj/18.18.5099.
31. Ernst J, Kellis M. ChromHMM: automating chromatin-state discovery and characterization. *Nat Methods*. 2012;9:215–216. doi: 10.1038/nmeth.1906.
32. Bogu GK, Vizán P, Stanton LW, Beato M, Di Croce L, Marti-Renom MA. Chromatin and RNA maps reveal regulatory long noncoding RNAs in mouse. *Mol Cell Biol*. 2015;36:809–819. doi: 10.1128/MCB.00955-15.
33. Elgin SC, Reuter G. Position-effect variegation, heterochromatin formation, and gene silencing in Drosophila. *Cold Spring Harb Perspect Biol*. 2013;5:a017780. doi: 10.1101/cshperspect.a017780.
34. Taddei A, Maison C, Roche D, Almouzni G. Reversible disruption of pericentric heterochromatin and centromere function by inhibiting deacetylases. *Nat Cell Biol*. 2001;3:114–120. doi: 10.1038/35055010.
35. McLean CY, Bristor D, Hiller M, Clarke SL, Schaar BT, Lowe CB, Wenger AM, Bejerano G. GREAT improves functional interpretation of cis-regulatory regions. *Nat Biotechnol*. 2010;28:495–501. doi: 10.1038/nbt.1630.
36. Hill JA, Olson EN. Cardiac plasticity. *N Engl J Med*. 2008;358:1370–1380. doi: 10.1056/NEJMra072139.
37. Delgado-Olguín P, Huang Y, Li X, Christodoulou D, Seidman CE, Seidman JG, Tarakhovsky A, Bruneau BG. Epigenetic repression of cardiac progenitor gene expression by Ezh2 is required for postnatal cardiac homeostasis. *Nat Genet*. 2012;44:343–347. doi: 10.1038/ng.1068.
38. Nguyen AT, Xiao B, Neppl RL, Kallin EM, Li J, Chen T, Wang DZ, Xiao X, Zhang Y. Dot1l regulates dystrophin expression and is critical for cardiac function. *Genes Dev*. 2011;25:263–274. doi: 10.1101/gad.2018511.
39. Maron BJ, Maron MS. Hypertrophic cardiomyopathy. *Lancet*. 2013;381:242–255. doi: 10.1016/S0140-6736(12)60397-3.
40. Hohl M, Wagner M, Reil JC, Müller SA, Tauchnitz M, Zimmer AM, Lehmann LH, Thiel G, Böhm M, Backs J, Maack C. HDAC4 controls histone methylation in response to elevated cardiac load. *J Clin Invest*. 2013;123:1359–1370. doi: 10.1172/JCI61084.
41. Chang S, McKinsey TA, Zhang CL, Richardson JA, Hill JA, Olson EN. Histone deacetylases 5 and 9 govern responsiveness of the heart to a subset of stress signals and play redundant roles in heart development. *Mol Cell Biol*. 2004;24:8467–8476. doi: 10.1128/MCB.24.19.8467-8476.2004.
42. Haberland M, Montgomery RL, Olson EN. The many roles of histone deacetylases in development and physiology: implications for disease and therapy. *Nat Rev Genet*. 2009;10:32–42. doi: 10.1038/nrg2485.
43. Potthoff MJ, Olson EN. MEF2: a central regulator of diverse developmental programs. *Development*. 2007;134:4131–4140. doi: 10.1242/dev.008367.
44. Chow JC, Ciaudo C, Fazzari MJ, Mise N, Servant N, Glass JL, Attreed M, Avner P, Wutz A, Barillot E, Greally JM, Voinnet O, Heard E. LINE-1 activity in facultative heterochromatin formation during X chromosome inactivation. *Cell*. 2010;141:956–969. doi: 10.1016/j.cell.2010.04.042.
45. Gilsbach R, Preissl S, Grüning BA, Schnick T, Burger L, Benes V, Würch A, Bönisch U, Günther S, Backofen R, Fleischmann BK, Schübeler D, Hein L. Dynamic DNA methylation orchestrates cardiomyocyte development, maturation and disease. *Nat Commun*. 2014;5:5288. doi: 10.1038/ncomms6288.
46. Greco CM, Kunderfranco P, Rubino M, Larcher V, Carullo P, Anselmo A, Kurz K, Carell T, Angius A, Latronico MV, Papait R, Condorelli G. DNA hydroxymethylation controls cardiomyocyte gene expression in development and hypertrophy. *Nat Commun*. 2016;7:12418. doi: 10.1038/ncomms12418.
47. Massengill MT, Ashraf HM, Chowdhury RR, Chrzanowski SM, Kar J, Warren SA, Walter GA, Zeng H, Kang BH, Anderson RH, Moss RL, Kasahara H. Acute heart failure with cardiomyocyte atrophy induced in adult mice by ablation of cardiac myosin light chain kinase. *Cardiovasc Res*. 2016;111:34–43. doi: 10.1093/cvr/cvw069.
48. Warren SA, Briggs LE, Zeng H, Chuang J, Chang EI, Terada R, Li M, Swanson MS, Lecker SH, Willis MS, Spinale FG, Maupin-Furlowe J, McMullen JR, Moss RL, Kasahara H. Myosin light chain phosphorylation is critical for adaptation to cardiac stress. *Circulation*. 2012;126:2575–2588. doi: 10.1161/CIRCULATIONAHA.112.116202.
49. Ceci M, Gallo P, Santonastasi M, Grimaldi S, Latronico MV, Pitisci A, Missol-Kolka E, Scimia MC, Catalucci D, Hilfiker-Kleiner D, Condorelli G. Cardiac-specific overexpression of E40K active Akt prevents pressure overload-induced heart failure in mice by increasing angiogenesis and reducing apoptosis. *Cell Death Differ*. 2007;14:1060–1062. doi: 10.1038/sj.cdd.4402095.
50. Shiojima I, Sato K, Izumiya Y, Schiekofer S, Ito M, Liao R, Colucci WS, Walsh K. Disruption of coordinated cardiac hypertrophy and angiogenesis contributes to the transition to heart failure. *J Clin Invest*. 2005;115:2108–2118. doi: 10.1172/JCI24682.
51. Wang Z, Zhang XJ, Ji YX, Zhang P, Deng KQ, Gong J, Ren S, Wang X, Chen I, Wang H, Gao C, Yokota T, Ang YS, Li S, Cass A, Vondriska TM, Li G, Deb A, Srivastava D, Yang HT, Xiao X, Li H, Wang Y. The long noncoding RNA Chaer defines an epigenetic checkpoint in cardiac hypertrophy. *Nat Med*. 2016;22:1131–1139. doi: 10.1038/nm.4179.